

## Letter

# A new isomer in $^{136}\text{Ba}$ populated by deep inelastic collisions

T. Shizuma<sup>1,a</sup>, Z.G. Gan<sup>1,2</sup>, K. Ogawa<sup>3</sup>, H. Nakada<sup>3</sup>, M. Oshima<sup>1</sup>, Y. Toh<sup>1</sup>, T. Hayakawa<sup>1</sup>, Y. Hatsukawa<sup>1</sup>, M. Sugawara<sup>4</sup>, Y. Utsuno<sup>1</sup>, and Z. Liu<sup>2</sup>

<sup>1</sup> Japan Atomic Energy Research Institute, Tokai, Ibaraki, 319-1195, Japan

<sup>2</sup> Institute of Modern Physics, Chinese Academy of Science, Lanzhou 730000, PRC

<sup>3</sup> Chiba University, Inage-ku, Chiba 263-8522, Japan

<sup>4</sup> Chiba Institute of Technology, Narashino, Chiba 275-0023, Japan

Received: 22 September 2003 / Revised version: 11 November 2003 /

Published online: 6 April 2004 – © Società Italiana di Fisica / Springer-Verlag 2004

Communicated by D. Schwalm

**Abstract.** Excited states in  $^{136}\text{Ba}$ , populated in deep inelastic collisions by the interaction of 450 MeV  $^{82}\text{Se}$  ions with a  $^{139}\text{La}$  target, have been studied by means of in-beam  $\gamma$ -ray spectroscopy. A new isomer with  $I^\pi = (10^+)$  has been identified at an excitation energy  $E_x = 3.357$  MeV. The half-life was determined as  $T_{1/2} = 94 \pm 10$  ns. The extracted  $B(E2)$  value is much smaller than those in  $^{132}\text{Te}$  and  $^{134}\text{Xe}$ . This hindrance is investigated by a shell model calculation.

**PACS.** 21.10.Tg Lifetimes – 23.20.Lv  $\gamma$  transitions and level energies – 27.60.+j  $90 \leq A \leq 149$

The  $^{136}\text{Ba}_{80}$  nucleus lies near the neutron shell closure at  $N = 82$  and in the proton mid-shell between  $Z = 50$  and 64 shell closures. In this region, an interplay of quadrupole collectivity and single-particle degrees of freedom could exist even in the relatively low-lying states. The yrast  $10^+$  isomers have been observed in the  $N = 80$  isotones  $^{132}\text{Te}$  [1, 2],  $^{134}\text{Xe}$  [2] and  $^{138}\text{Ce}$  [3]. The  $\nu(h_{11/2})^{-2}$  configuration is expected to be dominant for these isomers. On the other hand, because of the quadrupole collectivity, other configurations can significantly mix in the low-spin yrast states including the states which the  $10^+$  isomers decay into. The decay rates as well as the excitation energies of the isomers are therefore important measures in understanding the nuclear structure in this region.

Since the yrast  $10^+$  isomers are known for  $^{132}\text{Te}$ ,  $^{134}\text{Xe}$  and  $^{138}\text{Ce}$ , a similar  $10^+$  isomer is expected for the  $N = 80$  isotone of  $^{136}\text{Ba}$ . However, no evidence for such a state has been reported so far, primarily due to experimental difficulties to access higher-spin states in this nucleus. In this paper we report on the first identification of the  $10^+$  isomer in  $^{136}\text{Ba}$ , which was done by a deep-inelastic-collision experiment. The half-life of the isomer was measured by use of the  $\gamma$ - $\gamma$  coincidence method. A remarkable hindrance of the  $E2$  transition strength compared with those

for the neighboring nuclei of  $^{132}\text{Te}$  and  $^{134}\text{Xe}$  is found and will be discussed based on a shell model calculation.

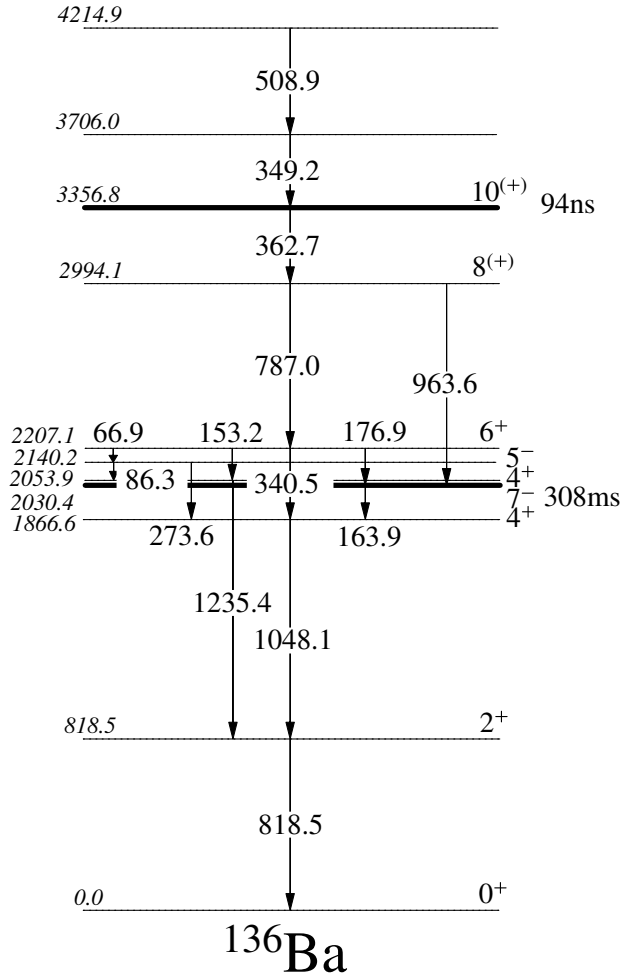
During the process of this work, we have noticed an independent study on  $^{136}\text{Ba}$  [4], where consistent results to this work were obtained.

In the present experiment, excited states in  $^{136}\text{Ba}$  have been produced in deep inelastic collisions (DIC) of  $^{82}\text{Se}$  ions with a  $^{139}\text{La}$  target. The 450 MeV  $^{82}\text{Se}$  beam was supplied by the tandem accelerator at the Japan Atomic Energy Research Institute (JAERI). The thick self-supporting target with a thickness of 100 mg/cm<sup>2</sup> was used to stop recoiled residuals inside the target material. Emitted  $\gamma$ -rays were detected by the GEMINI detector array, consisting of 12 Compton-suppressed HP-Ge detectors. The detectors were positioned at angles of 32° (2 detectors), 58° (2), 90° (4), 122° (2) and 148° (2) relative to the beam direction. A typical energy resolution of the Ge detectors was 2.4 keV at 1.33 MeV of  $^{60}\text{Co}$ . Energies and a relative time of  $\gamma$ -rays were recorded on magnetic tapes when two or more Ge detectors were detected in coincidence. The coincidence time window was set to 200 ns so that half-lives of less than  $\sim 100$  ns could be extracted. A total of  $3 \times 10^7$   $\gamma$ - $\gamma$  events were collected. The energy calibration was made by using  $^{133}\text{Ba}$  and  $^{152}\text{Eu}$  standard sources. Two-dimensional  $\gamma$ - $\gamma$  matrices of both prompt-prompt and prompt-delayed coincidences were created to construct the level scheme.

<sup>a</sup> e-mail: shizuma@popsvr.tokai.jaeri.go.jp

**Table 1.** Energies, level assignments, relative intensities, and DCO ratios for the  $\gamma$ -ray transitions in  $^{136}\text{Ba}$ .

$E_\gamma$ (keV)	$E_i$ (keV)	$J_i^\pi \rightarrow J_f^\pi$	$I_\gamma$	DCO
66.9(1)	2207.1	$6^+ \rightarrow 5^-$	11(1)	
86.3(1)	2140.2	$5^- \rightarrow 4^+$	6(1)	
153.2(1)	2207.1	$6^+ \rightarrow 4^+$	7(1)	0.7(1)
163.9(1)	2030.4	$7^- \rightarrow 4^+$	12(1)	0.6(1)
176.9(1)	2207.1	$6^+ \rightarrow 7^-$	16(1)	0.7(1)
273.6(1)	2140.2	$5^- \rightarrow 4^+$	13(1)	0.8(1)
340.5(1)	2207.1	$6^+ \rightarrow 4^+$	48(2)	0.9(1)
349.2(2)	3706.0	$\rightarrow 10^{(+)}$	70(2)	
362.7(1)	3356.8	$10^{(+)}$ $\rightarrow$ $8^{(+)}$	46(2)	0.9(1)
508.9(1)	4214.9		40(2)	
787.0(1)	2994.1	$8^{(+)}$ $\rightarrow$ $6^+$	85(3)	0.9(1)
818.5(1)	818.5	$2^+ \rightarrow 0^+$	100(3)	1.2(1)
963.6(1)	2994.1	$8^{(+)}$ $\rightarrow$ $7^-$	8(1)	
1048.1(1)	1866.6	$4^+ \rightarrow 2^+$	75(3)	1.0(1)
1235.4(1)	2053.9	$4^+ \rightarrow 2^+$	25(2)	1.0(1)

**Fig. 1.** A proposed level scheme of  $^{136}\text{Ba}$ .

The directional correlations of  $\gamma$ -rays de-exciting oriented states (DCO) ratio [5, 6] defined below was used to

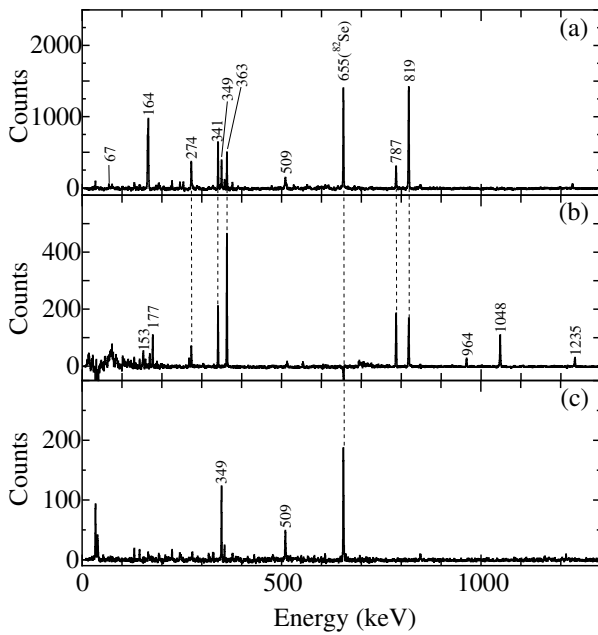
deduce transition multipole orders:

$$R_{\text{DCO}} = \frac{I_\gamma \text{ at } 32^\circ (\text{or } 148^\circ) \text{ gated on } \gamma_G \text{ at } 90^\circ}{I_\gamma \text{ at } 90^\circ \text{ gated on } \gamma_G \text{ at } 32^\circ (\text{or } 148^\circ)}.$$

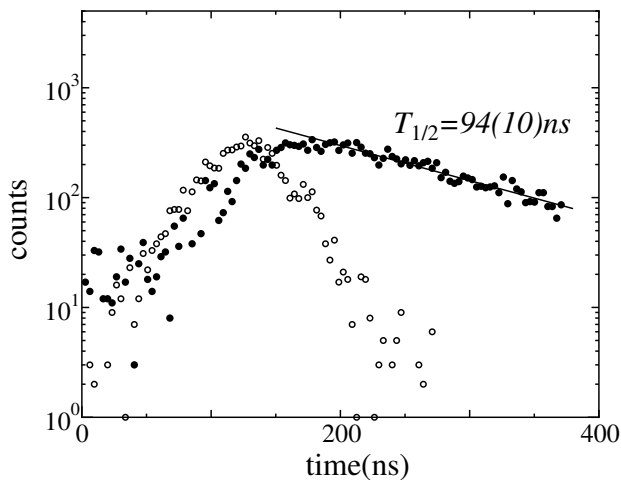
Since the angle of  $148^\circ$  is equivalent to that of  $32^\circ$  [6], the corresponding events were summed in the DCO matrices to increase the statistics. In the DCO analysis, stretched  $\Delta I = 2$  transitions close to the  $\gamma$ -ray of interest are generally used as gates ( $\gamma_G$ ). In this case, the DCO ratios fall into unity for stretched quadrupole ( $\Delta I = 2$ ) and unstretched dipole ( $\Delta I = 0$ ) transitions, while the values are  $\sim 0.6$  for stretched dipole ( $\Delta I = 1$ ) transitions. For mixed  $\Delta I = 1$  transitions, the DCO ratios depend on the mixing ratio  $\delta$ .

Figure 1 shows a level scheme of  $^{136}\text{Ba}$  resulting from the present work. The transition energies,  $\gamma$ -ray intensities and DCO ratios are also summarized in table 1. The transitions below the 2207 keV state were previously known [7]. A 787 keV  $\gamma$ -ray seen in fig. 2(a) which is obtained by gating on the 1048 keV  $4^+ \rightarrow 2^+$  transition connects the 2207 keV and 2994 keV level [8]. In the present work, a 964 keV crossover transition depopulating the 2994 keV level was newly observed. In addition, three new transitions with energies of 349, 363 and 509 keV were found in coincidence with the lower-lying transitions in  $^{136}\text{Ba}$ . From the analysis of the prompt-delayed coincidence spectra (figs. 2(b) and (c)), a new isomer was identified at  $E_x = 3357$  keV, decaying to the 2994 keV level via the 363 keV transition. The transitions below the isomer can be seen in the delayed spectrum (fig. 2(b)). Above the isomer, the 349 and 509 keV transitions were also observed (fig. 2(c)). The DCO ratios for the 363 and 787 keV transitions are consistent with  $\Delta I = 2$ , resulting in assignments of  $I = 8$  for the 2994 keV state and  $I = 10$  for the 3357 isomeric state. The positive-parity assignments are preferred by the systematic behavior of the yrast  $8^+$  and  $10^+$  energy levels in the region.

For the determination of the half-life of the  $10^+$  isomer, a  $\gamma$ -ray time difference spectrum has been analyzed. Figure 3 shows a decay curve of the isomer. By



**Fig. 2.** (a) A prompt coincidence spectrum gated on the 1048 keV transition. A delayed  $\gamma$ -ray spectrum gated on the 349 keV transition, showing  $\gamma$ -rays below the  $10^+$  isomer is also drawn in panel (b), while an early  $\gamma$ -ray spectrum gated on the 819 and 1048 keV transitions, showing the transitions above the  $10^+$  isomer, is drawn in panel (c).



**Fig. 3.** A time difference spectrum between the 349 keV transition and the 340, 363, 787, 819, 1048 keV transitions, showing the decay curve for the isomer. The time difference spectrum in prompt coincidence is also shown with open circles.

fitting the decay slope, the half-life was determined as  $T_{1/2} = 94(10)$  ns. Assuming that the 363 keV transition has a pure  $E2$  character, the reduced  $E2$  transition probability is extracted as  $B(E2) = 0.96(10) e^2\text{fm}^4$ . This value is much smaller than those for the neighboring nuclei of  $^{132}\text{Te}$ ,  $B(E2) = 42(1) e^2\text{fm}^4$  and  $^{134}\text{Xe}$ ,  $B(E2) = 26(5) e^2\text{fm}^4$  [2]. The energy levels and the  $E2$  strength of the  $10^+$  isomers will be discussed in the next section based on a shell model calculation.

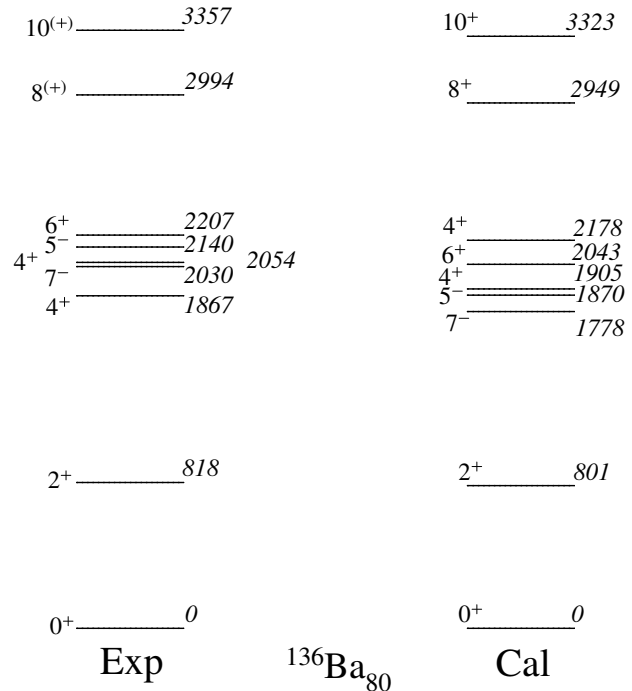


**Fig. 4.** Comparison of experimental and calculated energy levels of  $^{136}\text{Ba}$ .

In order to investigate the  $E2$  strength of the  $10^+$  isomer observed in  $^{136}\text{Ba}$ , a shell model calculation has been carried out. We take the  $(0g_{7/2}1d_{5/2}2s_{1/2}0h_{11/2}1d_{3/2})$  orbits for protons and  $(2s_{1/2}0h_{11/2}1d_{3/2})$  for neutron holes, on top of the  $^{132}\text{Sn}$  inert core. For protons, the excitation out of  $(0g_{7/2}1d_{5/2})$  is restricted up to 4 particles with the total seniority  $v \leq 4$ . We adopt the surface delta-interaction (SDI) for the  $pp$  and  $nn$  interaction, whose strengths as well as the single-particle energies are fitted to the observed levels of  $^{134}\text{Te}$  and  $^{130}\text{Sn}$ . The quadrupole-quadrupole interaction is used for the  $pn$  interaction. The excitation energies of the  $8^+$  and  $10^+$  states are rather sensitive to the single-hole energy of  $n0h_{11/2}$  in this region. Although the attractive monopole  $pn$  interaction plays a certain role, the present schematic interaction may not treat this effect properly. We therefore introduce a slight  $Z$ -dependence of the single-hole energy so as to reproduce the levels of the neighboring  $N = 81$  nuclei. Note that this shift of the single-hole energy does not influence significantly the  $E2$  strengths of the  $10^+$  isomers shown below. The calculated energy levels of  $^{136}\text{Ba}$  are presented in fig. 4. The energy levels up to the  $10^+$  isomer are well reproduced.

In the calculation of the  $E2$  strengths, we use the effective charges  $e_p^{\text{eff}} = 2.8e$  and  $e_n^{\text{eff}} = 0.4e$ , which are fitted to  $B(E2; 2^+ \rightarrow 0^+)$  of the  $N = 82$  and  $80$  nuclei, as shown in table 2. The value of  $e_p^{\text{eff}}$  is somewhat larger than other shell model calculations in this region [9]. This may be ascribed to the truncation of the model space. With the effective charges fixed by the low-lying states, the  $E2$  decay strengths of the  $10^+$  isomers in the  $N = 80$  nuclei tend to be overestimated. However, the overall trend of

**Table 2.** Calculated  $B(E2; 2_1^+ \rightarrow 0_1^+)$  values ( $e^2\text{fm}^4$ ) of  $N = 82$  and  $80$  nuclei. Experimental data are taken from refs. [10, 11].

Nucleus	Experimental	Calculated
$^{134}_{52}\text{Te}_{82}$	–	209
$^{136}_{54}\text{Xe}_{82}$	$402 \pm 16$	357
$^{138}_{56}\text{Ba}_{82}$	$460 \pm 18$	436
$^{132}_{54}\text{Te}_{80}$	–	316
$^{134}_{54}\text{Xe}_{80}$	$680 \pm 120$	600
$^{136}_{56}\text{Ba}_{80}$	$820 \pm 16$	818

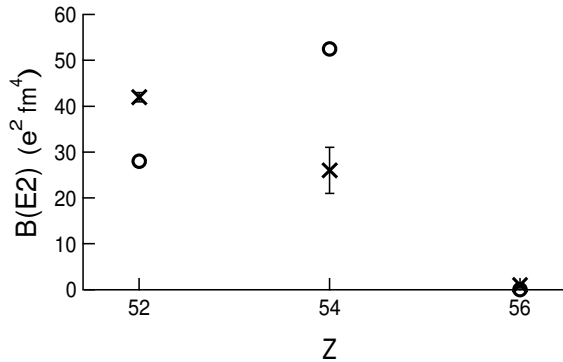


**Fig. 5.**  $B(E2)$  values from the  $10^+$  isomers for the  $N = 80$  isotones. The experimental values are shown by crosses with error bars, whereas the shell model values (scaled by  $1/2$ ) are shown by circles.

the  $B(E2)$  values, particularly the  $Z$ -dependence, is well reproduced. The measured and calculated  $E2$  strengths of the  $10^+$  isomers are depicted in fig. 5, where the calculated  $E2$  strengths are scaled by  $1/2$ .

Whereas it is not easy to reproduce accurately the  $B(E2)$  values of non-collective  $E2$  transitions, such as those of the  $10^+$  isomers, their  $Z$ -dependence seems to carry valuable information of nuclear structure [12]. The  $E2$  decay strength of  $10^+$  is remarkably hindered in  $^{136}\text{Ba}$  from those in  $^{132}\text{Te}$  and  $^{134}\text{Xe}$ . In analyzing the shell

model results, it is found that this hindrance originates from different characters of the wave functions between the  $10^+$  and  $8^+$  states. The  $10^+$  state is dominated by the  $J_p = 0, J_n = 10$  component, while the  $8^+$  state by the  $J_p = 2, J_n = 6$  component, and the  $E2$  transition matrix element between these components vanishes. Thus, the mismatch of configuration in the yrast states seems to account for the large retardation of the  $E2$  transition from the  $10^+$  isomer observed in  $^{136}\text{Ba}$ .

We have firstly identified a  $10^+$  isomer in  $^{136}\text{Ba}$ . The half-life of the isomer was measured as  $94(10)$  ns corresponding to  $B(E2) = 0.96(10) e^2\text{fm}^4$  for the  $10^+ \rightarrow 8^+$  transition. A shell model calculation has been carried out to investigate the  $E2$  strength of the  $10^+$  isomers in  $^{136}\text{Ba}$  and its neighbours. The hindrance for the isomeric transition in  $^{136}\text{Ba}$  has been attributed to the different characters of the wave functions of the  $10^+$  and  $8^+$  states.

We would like to thank the staff of the JAERI tandem accelerator for providing the ion beam. This work is supported by STA Exchange Program and by NSFC-19705011, NSFC-19905012.

## References

1. K. Sistemich *et al.*, *Z. Phys. A* **292**, 45 (1979).
2. J. Genevey *et al.*, *Phys. Rev. C* **63**, 054315 (2001).
3. A.M. Morozov *et al.*, *Sov. Phys. JETP* **12**, 674 (1961).
4. J.J. Valiente-Dobón, P.H. Regan *et al.*, private communication (2003); J.J. Valiente-Dobón *et al.*, *Phys. Rev. C* **69**, 024316 (2004).
5. K.S. Krane *et al.*, *Nucl. Data Tables* **11**, 351 (1973).
6. L.P. Ekström, A. Nordlund, *Nucl. Instrum. Methods A* **313**, 421 (1992).
7. A.R. Farlan *et al.*, *Nucl. Data Sheets* **71**, 1 (1994).
8. E. Dragulescu *et al.*, *Rev. Roum. Phys.* **32**, 743 (1987).
9. L. Eßer *et al.*, *Nucl. Phys. A* **672**, 111 (2001).
10. G. Jakob *et al.*, *Phys. Rev. C* **65**, 024316 (2002).
11. S. Raman *et al.*, *At. Data Nucl. Data Tables* **78**, 1 (2001).
12. T. Matsuzawa *et al.*, *Phys. Rev. C* **62** 054304 (2000); **63** 029902(E) (2001).